

Gauge invariance of radiative jet functions in the position-space formulation of SCET

Geoffrey T. Bodwin,^{1,*} June-Haak Ee,^{2,†} Daekyoung Kang,^{2,‡} and Xiang-Peng Wang^{3,§}

¹*High Energy Physics Division, Argonne National Laboratory, Argonne, Illinois 60439, USA*

²*Key Laboratory of Nuclear Physics and Ion-beam*

Application (MOE) and Institute of Modern Physics,

Fudan University, Shanghai 200433, China

³*Technical University of Munich, TUM School of Natural Sciences,*

Department of Physics T30f, James-Franck-Straße 1, 85748 Garching, Germany

(Dated: April 2, 2024)

Abstract

In subleading powers of soft-collinear effective theory (SCET), the Lagrangian contains couplings between soft quarks and hard-collinear quarks. Matrix elements of the hard-collinear parts of these couplings are radiative jet functions. In the position-space formulation of SCET, the Lagrangians are constructed from operators that appear to be gauge invariant. Nevertheless, we find violations of gauge invariance arise in the hard-collinear sector because gauge transformations can shift the momentum of a hard-collinear quark field from the hard-collinear sector to the soft sector, where the hard-collinear fields, by definition, have no support. The violations of gauge invariance are manifested in perturbation theory in the hard-collinear sector through the absence of certain Feynman diagrams that would be present in full QCD. A consequence of the absence of these diagrams is that the radiative jet functions that follow directly from the position-space Lagrangians are not gauge invariant, and we demonstrate this through explicit calculations in lower-order perturbation theory. We obtain gauge-invariant Lagrangians by adding to existing position-space Lagrangians terms that are proportional to the soft-quark equation of motion. These gauge-invariant Lagrangians are valid for nonzero, as well as zero, quark masses. We also remark briefly on the gauge invariance of certain Lagrangians that have been constructed in the label-momentum formulation of SCET.

* gtb@anl.gov

† june_haak_ee@fudan.edu.cn

‡ dkang@fudan.edu.cn

§ xiangpeng.wang@tum.de

I. INTRODUCTION

In soft-collinear effective theory (SCET) [1–5], couplings between a quark that carries a soft momentum and a quark that carries a hard-collinear momentum appear in subleading powers of the SCET expansion parameter λ [6–9]. Matrix elements that contain the hard-collinear parts of these couplings are called “radiative jet functions,” and they appear in factorization theorems for exclusive processes at subleading power in λ . (See, for example, Refs. [10–12].)

In general, radiative jet functions are written in terms of operators in which hard-collinear quark and antiquark fields are accompanied by Wilson-line factors, and all derivatives are covariant derivatives. We call such operators “ostensibly gauge-invariant operators.” If one replaces the hard-collinear quark and antiquark fields with full QCD fields multiplied by collinear projectors, then the ostensibly gauge-invariant operators are truly gauge invariant. However, in SCET, the hard-collinear quark and antiquark fields must carry hard-collinear momenta, not soft momenta.¹ This requirement can lead to violations of hard-collinear gauge invariance because hard-collinear gauge transformations multiply quark fields by a phase that, in momentum space, can shift the quark-field momentum from the hard-collinear region to the soft region, where the hard-collinear fields have no support. As we will see, this phenomenon is manifested diagrammatically by the absence of certain Feynman diagrams in the hard-collinear sector that would be present in full QCD. These “missing diagrams” can lead to violations of gauge invariance in the hard-collinear sector.

We carry out an analysis of the Lagrangians that appear in the position-space formulation of SCET in Refs. [6, 7], which we refer to as Beneke-Chapovsky-Diehl-Feldmann (BCDF).² We demonstrate, through the use of Ward identities, that the BCDF Lagrangians lead to violations of gauge invariance in the hard-collinear sector. The violations occur in order λ^2 , but not in order λ^1 . We find that the violations of gauge invariance can be removed by making use of the soft-quark equation of motion. Therefore, the BCDF Lagrangians lead to gauge-invariant S -matrix elements [13]. However, off-shell quantities, such as radiative jet functions can be gauge noninvariant. We use the Lagrangians in Refs. [6, 7] directly

¹ The requirement that hard-collinear quark and gluon fields carry hard-collinear momenta is essential in working out SCET power counting and in achieving a factorization of the hard-collinear sector of the effective theory from the other sectors at the Lagrangian level. The assumption that the hard-collinear quark and gluon fields carry hard-collinear momenta is used explicitly in Refs. [6, 7] in constructing the Lagrangians in those papers.

² The Lagrangians in Eq. (A.1) of Ref. [12] are the BCDF Lagrangians, but expressed in terms of gauge-invariant building blocks. In this paper, we carry out our analyses in terms of the original BCDF forms of the Lagrangians.

to construct radiative jet functions. That is, we define the radiative jet functions as time-ordered matrix elements of the hard-collinear-operator factors in the Lagrangians. We find, through explicit calculations at the lowest nontrivial order in perturbation theory, that the resulting radiative jet functions are not gauge invariant.

We modify the BCDF Lagrangians to obtain gauge-invariant Lagrangians that describe the couplings of a soft quark to a hard-collinear quark by applying the soft-quark equation of motion and by making use of the Bauer-Pirjol-Stewart (BPS) field redefinition in Ref. [4] to factor minus-polarized soft gluons from the hard-collinear subdiagram. We use the concept of missing diagrams to argue that the modified order- λ^2 Lagrangians, as well as the order- λ^1 Lagrangian, are gauge invariant to all orders in perturbation theory. We also demonstrate the gauge invariance by using the modified order- λ^2 Lagrangians to construct radiative jet functions and computing the radiative jet functions in the Feynman gauge and the light-cone gauge at the lowest nontrivial order in perturbation theory.

In the label-momentum formulation of SCET [2], the Lagrangians that describe the interactions of soft quarks with hard-collinear quarks are also constructed from ostensibly gauge-invariant operators [3]. We find that the label-momentum Lagrangians in Refs. [8, 9] evade the gauge invariance issue that we identify in this paper and that the corresponding operators are truly gauge invariant.

The remainder of this paper is organized as follows. In Sec. II, we establish the notations and conventions that we use throughout this paper. In Sec. III, we present the Lagrangians of Refs. [6, 7], discuss the associated Ward identities in lowest-order perturbation theory, and identify the sources of violations of gauge invariance as the “missing diagrams.” In Sec. IV, we use the BCDF Lagrangians to compute radiative jet functions in the Feynman gauge and in the light-cone gauge at lowest order in perturbation theory, and we show that these two gauges give different results, verifying the violation of gauge invariance. In Sec. V we modify the BCDF Lagrangians at relative order λ^2 to obtain gauge-invariant Lagrangians that connect a soft quark to a hard-collinear quark. In Sec. VI, we argue that the order- λ^1 Lagrangian and the modified order- λ^2 Lagrangians are gauge invariant to all orders in perturbation theory. We construct radiative jet functions that follow from the modified gauge-invariant Lagrangians in Sec. VII, and we calculate these radiative jet functions in the Feynman gauge and in the light-cone gauge in lowest-order perturbation theory, verifying that the radiative jet functions are invariant with respect to these gauge

choices. In Sec. VIII, we observe that certain versions of the label-momentum formulation of SCET evade the gauge-invariance problem that we identify in this paper. Finally, we summarize and discuss our results in Sec. IX.

II. PRELIMINARIES

In this section, we establish the notations and conventions that we use throughout this paper.

We decompose an arbitrary vector in terms of the two lightlike vectors, n and \bar{n} , as follows:

$$r^\mu = r^- \frac{\bar{n}^\mu}{2} + r^+ \frac{n^\mu}{2} + r_\perp^\mu, \quad (1)$$

where

$$r^+ = \bar{n} \cdot r, \quad r^- = n \cdot r, \quad r_\perp^\mu = r^\mu - r^- \frac{\bar{n}^\mu}{2} - r^+ \frac{n^\mu}{2}, \quad (2)$$

with $n^2 = \bar{n}^2 = 0$ and $n \cdot \bar{n} = 2$. n and \bar{n} are the lightlike unit vectors along the z axis:

$$n^\mu = (1, 0, 0, 1), \quad \bar{n}^\mu = (1, 0, 0, -1). \quad (3)$$

The perpendicular momentum r_\perp^μ satisfies $n \cdot r_\perp = \bar{n} \cdot r_\perp = 0$. Here, and throughout this paper, we use the notation

$$r_\perp^2 = -\mathbf{r}_\perp^2, \quad (4)$$

where \mathbf{r}_\perp is a $(D - 2)$ -dimensional Euclidean vector.

It is convenient to consider the case of a quark with mass $m \gg \Lambda_{\text{QCD}}$. Then, a soft momentum r_s on the quark line has the scaling behavior

$$r_s^+ \sim Q\lambda^2, \quad r_s^- \sim Q\lambda^2, \quad r_{s\perp} \sim Q\lambda^2, \quad (5)$$

where ³

$$\lambda = \sqrt{\frac{m}{Q}}, \quad (6)$$

and Q is the hard scale of the process. A collinear momentum r_c on the quark line along the n direction has the scaling behavior

$$r_c^+ \sim Q, \quad r_c^- \sim Q\lambda^4, \quad r_{c\perp} \sim Q\lambda^2. \quad (7)$$

Since a radiative jet function carries a soft momentum combined with a collinear momentum, the resulting hard-collinear momentum r_{hc} , taken to be along the n direction, has the scaling behavior ⁴

$$r_{hc}^+ \sim Q, \quad r_{hc}^- \sim Q\lambda^2, \quad r_{hc\perp} \sim Q\lambda. \quad (8)$$

Note that the hard-collinear and soft momenta have different virtualities in λ : $r_{hc}^2 \sim Q^2\lambda^2$, and $r_s^2 \sim Q^2\lambda^4$.

The n -hard-collinear Dirac field ψ_n can be decomposed into large- and small-component collinear fields by applying collinear projectors P_n and $P_{\bar{n}}$ onto ψ_n :

$$\xi_n = P_n\psi_n, \quad (9a)$$

$$\eta_n = P_{\bar{n}}\psi_n, \quad (9b)$$

where

$$P_n = \frac{\not{n}\not{\bar{n}}}{4}, \quad P_{\bar{n}} = \frac{\not{\bar{n}}\not{n}}{4}. \quad (10)$$

We make use of the following additional notations for SCET fields: q_s is a soft-quark field, G_n^μ is an n -hard-collinear-gluon field, and G_s^μ is a soft-gluon field. q_s , η_n and ξ_n have scaling of order λ^3 , λ^2 and λ , respectively. Each component of the field G_n^μ has the same scaling as the n -hard-collinear momentum in Eq. (8), and each component of the field G_s^μ has the same scaling as the soft momentum in Eq. (5). $g_s = \sqrt{4\pi\alpha_s}$ is the strong coupling.

³ Our general arguments and specific examples are also valid for massless quarks for those cases that do not involve an interaction between a soft-quark and a hard-collinear quark that is proportional to m . In the massless case, the SCET scaling parameter is $\lambda = (\Lambda_{\text{QCD}}/Q)^{1/2}$.

⁴ The scaling of $r_{hc\perp}$ is chosen so that $r_{hc\perp}^2 \sim r_{hc}^+ r_{hc}^-$.

We define the n -hard-collinear Wilson line as

$$W_n(x) = P \exp \left[ig_s \int_{-\infty}^0 ds \bar{n} \cdot G_n(x + s\bar{n}) \right], \quad (11)$$

and we define the covariant derivatives as

$$\begin{aligned} D^\mu &= \partial^\mu - ig_s G_n^\mu(x) - ig_s \bar{n} \cdot G_n(x^+) \frac{\bar{n}^\mu}{2}, \\ D_n^\mu &= \partial^\mu - ig_s G_n^\mu(x), \\ D_s^\mu &= \partial^\mu - ig_s G_s^\mu(x). \end{aligned} \quad (12)$$

III. WARD IDENTITIES OF THE BCDF SCET LAGRANGIANS

A. BCDF Lagrangians

The effective Lagrangians that describe an interaction between a soft quark q_s and an n -hard-collinear quark ξ_n in the SCET formulation Refs. [6, 7] are given by

$$\mathcal{L}_1^{\text{BCDF}}(x) = \bar{q}_s(x^+) (W_n^\dagger i \not{D}_{n\perp} \xi_n)(x) + \text{H.c.}, \quad (13a)$$

$$\mathcal{L}_{2a}^{\text{BCDF}}(x) = \bar{q}_s(x^+) \left\{ W_n^\dagger \left(in \cdot D + i \not{D}_{n\perp} \frac{1}{i\bar{n} \cdot D_n} i \not{D}_{n\perp} \right) \frac{\not{n}}{2} \xi_n \right\} (x) + \text{H.c.}, \quad (13b)$$

$$\mathcal{L}_{2b}^{\text{BCDF}}(x) = \left[\bar{q}_s(-i \overleftarrow{D}_{s\perp}^\rho) \right] (x^+) (ix_{\perp\rho} W_n^\dagger i \not{D}_{n\perp} \xi_n)(x) + \text{H.c.}, \quad (13c)$$

$$\mathcal{L}_{2m}^{\text{BCDF}}(x) = \bar{q}_s(x^+) (-m W_n^\dagger \xi_n)(x) + \text{H.c.}, \quad (13d)$$

where H.c. denotes the Hermitian conjugate, and the subscripts 1 and 2 indicate the order in λ of these expressions. These Lagrangians generalize slightly those in Refs. [6, 7], in that they contain a nonzero quark mass. However, we refer to them as the BCDF Lagrangians. In deriving these expressions, we have started in full QCD, with a quark with mass m , and we have followed the steps that are given in Refs. [6, 7] for the massless case. The detailed derivation of $\mathcal{L}_{2m}^{\text{BCDF}}$ is given in Appendix A.

References [6, 7] also contain the $\bar{\xi}_n \dots \xi_n$, $\bar{q}_s \dots q_s$, and pure gauge-field SCET Lagrangians. The modifications of these Lagrangians for the massive case at orders λ^0 , λ^1 , and λ^2 are also shown in Appendix A. In this paper, we do not use these Lagrangians explicitly. Instead, we employ an equivalent, but simpler, procedure: we replace the fields ξ_n and $\bar{\xi}_n$

with hard-collinear Dirac fields, using the expressions in Eq. (9); we use full-QCD Feynman rules, with the projectors P_n and $P_{\bar{n}}$; and we expand to the desired order in λ .

The power counting in λ in Eq. (13) follows from the fact that, if we integrate the interaction Lagrangians in Eq. (13) over d^4x , then the integration region is of order λ^{-4} . In $\mathcal{L}_{2b}^{\text{BCDF}}(x)$, the factor $ix_{\perp\rho}$ should be counted as $O(\lambda^{-1})$ because it scales as the inverse of the transverse momentum that flows into the hard-collinear subdiagram.

Note that, in Eq. (13), the soft-quark field q_s depends only on x^+ . That is, the soft-quark field has been multipole expanded in the minus and transverse components of its argument in order to obtain a definite scaling in λ [6]. Square brackets indicate that a derivative acts only inside the brackets and that soft fields are evaluated at x^+ after the derivative is taken.

The factor $ix_{\perp\rho}$ becomes, in momentum space, a derivative with respect to the transverse component of the soft momentum. In momentum space, the multipole expansion of q_s implies that the plus and transverse components of the soft momentum are ultimately set to zero, but only after derivatives with respect to the soft momentum have been taken.

At this stage, minus-polarized soft gluons still attach to the hard-collinear subdiagram. These attachments can be factored into Wilson lines by making use of the Grammer-Yennie approximation [14], followed by the application of perturbative Ward identities [15]. Equivalently, the decoupling can be achieved by making use of the BPS collinear-field redefinitions [4]:

$$\xi_n(x) \rightarrow S_n(x^+) \xi_n(x), \quad G_n^\mu(x) \rightarrow S_n(x^+) G_n^\mu(x) S_n^\dagger(x^+), \quad (14)$$

where S_n is the soft Wilson line, which is defined by

$$S_n(x) = P \exp \left[ig_s \int_{-\infty}^0 dt n \cdot G_s(x + tn) \right]. \quad (15)$$

The net effect of the BPS field redefinitions is to make the simple replacements $\bar{q}_s(x^+) \rightarrow \bar{q}_s(x^+) S_n(x^+)$, $[\bar{q}_s(-i\overleftarrow{D}_{s\perp}^\rho)](x^+) \rightarrow [\bar{q}_s(-i\overleftarrow{D}_{s\perp}^\rho)](x^+) S_n(x^+)$, and $in \cdot D \rightarrow in \cdot D_n$ in Eq. (13). Note that the arguments of the soft Wilson lines have been multipole expanded to lowest order in λ , and, so, it is still true that only the minus component of the soft momentum enters the momentum-space expressions that derive from the BPS-transformed Lagrangians.

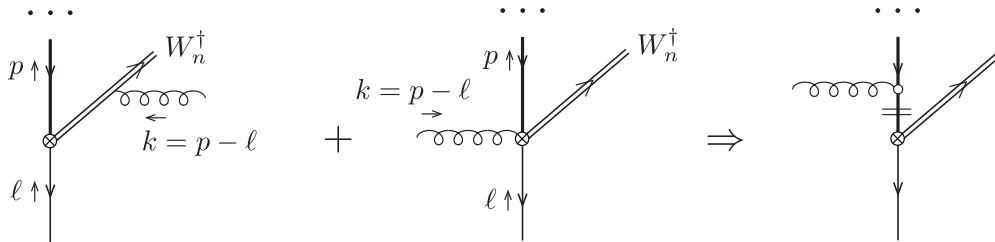


FIG. 1. Feynman diagrams showing a Ward identity for the operators in Eq. (13). The Ward identity is for the case in which a gluon attaches to the Wilson line (W_n^\dagger) or to the crossed circle (\otimes). The thick, solid line denotes a quark line that has a hard-collinear momentum ($-p$), and the solid line denotes a quark line that has a soft momentum ($-\ell$). The diagram on the right side of the arrow shows the contribution of the term k^μ in the gauge transformation in Eq. (19). The short, double lines across a propagator indicate that the propagator has been canceled.

B. Gauge invariance and Ward identities

At first sight, the hard-collinear parts of the interactions in Eq. (13) would appear to be gauge invariant with respect to gauge transformation of the hard-collinear fields. We can use Eq. (9a) to replace ξ_n with ψ_n . Then, if we could replace ψ_n with the ordinary Dirac field ψ , the hard-collinear parts of the interactions in Eq. (13) would be gauge-invariant full-QCD operators. However, as we will see, the restriction that ψ_n (and ξ_n) carry n -hard-collinear momenta implies that certain full-QCD diagrams are missing in hard-collinear functions involving these operators and that, consequently, the hard-collinear functions are not gauge invariant.

In order to investigate the gauge invariance of the $O(\lambda^2)$ SCET Lagrangians in Eq. (13), let us consider the interactions that follow from these Lagrangians in order g_s . The corresponding Feynman diagrams are shown on the left sides of Fig. 1. We imagine that these explicit interactions are embedded in a radiative jet function, whose remaining factors are indicated by an ellipsis in the figures and in the corresponding equations. In these figures, the quark momentum $-p$ is an n -hard-collinear momentum, the quark momentum $-\ell$ is a soft momentum, and the gluon momentum $k = p - \ell$ is an n -hard-collinear momentum. The crossed circles in Fig. 1 arise from the covariant-derivative and x_\perp factors in the Lagrangians. Their Feynman rules are given in Figs. 2 and 3. The order- g_s^0 contributions to the crossed

The figure shows two Feynman diagrams for crossed circles. The left diagram shows a Wilson line with a crossed circle, momentum p to the right, and a vertical arrow labeled $\ell^- \frac{\bar{n}}{2}$ pointing up. The right diagram is identical but includes a gluon line $G_n^{\mu,A}$ attached to the top of the crossed circle.

$$\begin{aligned}
V_1^{(0)} &= -\not{p}_\perp & V_1^{(1)} &= g_s T^A \gamma_{\perp\mu} \\
V_{2a}^{(0)} &= -\left(n \cdot p + \frac{p_\perp^2}{\bar{n} \cdot p}\right) \frac{\not{n}}{2} & V_{2a}^{(1)} &= g_s T^A \left(n_\mu + \gamma_{\perp\mu} \frac{\not{p}_\perp}{\bar{n} \cdot p}\right) \frac{\not{n}}{2} \\
V_{2m}^{(0)} &= -m & V_{2m}^{(1)} &= 0
\end{aligned}$$

FIG. 2. The Feynman rules for the crossed circles in Fig. 1 for the Lagrangians in Eqs. (13a), (13b), and (13d). V_1 , V_{2a} , and V_{2m} are the crossed-circle contributions that arise from $\mathcal{L}_1^{\text{BCDF}}$, $\mathcal{L}_{2a}^{\text{BCDF}}$, and $\mathcal{L}_{2m}^{\text{BCDF}}$, respectively. The superscripts (0) and (1) denote the order- g_s^0 and g_s^1 contributions of the crossed circle, respectively.

The figure shows two Feynman diagrams for crossed circles. The left diagram shows a Wilson line with a crossed circle, momentum p to the right, and a vertical arrow labeled $\ell^- \frac{\bar{n}}{2} + \ell_\perp$ pointing up. The right diagram is identical but includes a gluon line $G_n^{\mu,A}$ attached to the top of the crossed circle.

$$\begin{aligned}
V_{2b}^{(0)} &= \ell_\perp^\rho \Delta_\rho^{\ell_\perp} (-\not{p}_\perp) & V_{2b}^{(1)} &= g_s T^A \ell_\perp^\rho \Delta_\rho^{\ell_\perp} \gamma_{\perp\mu}
\end{aligned}$$

FIG. 3. The Feynman rules for the crossed circles in Fig. 1 for the Lagrangians in Eq. (13c). V_{2b} describes the crossed-circle contribution that arises from $\mathcal{L}_{2b}^{\text{BCDF}}$. The superscripts (0) and (1) denote the order- g_s^0 and order- g_s^1 contributions of the crossed circle, respectively. The definition of the operator $\Delta_\rho^{\ell_\perp}$ is given in Eq. (17).

circles can appear only in conjunction with one or more hard-collinear gluons that attach to the Wilson line. Otherwise, hard-collinear momentum would not be conserved at the crossed circles. In deriving these Feynman rules, we make use of the identity

$$ix_{\perp\rho} = \int d^{D-2}\ell_\perp \frac{\partial}{\partial \ell_\perp^\rho} [\delta^{D-2}(\ell_\perp)] e^{-i\ell_\perp \cdot x_\perp}, \quad (16)$$

and we define the operator

$$\Delta_{\rho}^{\ell_{\perp}} \equiv \int d^{D-2} \ell_{\perp} \delta^{D-2}(\ell_{\perp}) \frac{\partial}{\partial \ell_{\perp}^{\rho}}, \quad (17)$$

which picks up the coefficient of ℓ_{\perp}^{ρ} .

The amplitudes for $\mathcal{L}_1^{\text{BCDF}}$, $\mathcal{L}_{2a}^{\text{BCDF}}$, $\mathcal{L}_{2b}^{\text{BCDF}}$, and $\mathcal{L}_{2m}^{\text{BCDF}}$, which correspond to the diagram in Fig. 1, are

$$\begin{aligned} A_1 &= \epsilon^{\mu}(k) \left[\frac{(-ig_s)(i)\bar{n}_{\mu}}{\bar{n} \cdot k + i\varepsilon} (-\not{p}_{\perp}) + g_s \gamma_{\perp\mu} \right] P_n \dots, \\ A_{2a} &= \epsilon^{\mu}(k) \left[\frac{(-ig_s)(i)\bar{n}_{\mu}}{\bar{n} \cdot k + i\varepsilon} \left(-n \cdot p - \frac{p_{\perp}^2}{\bar{n} \cdot p} \right) + g_s \left(n_{\mu} + \gamma_{\perp\mu} \frac{\not{p}_{\perp}}{\bar{n} \cdot p} \right) \right] \frac{\not{n}}{2} P_n \dots, \\ A_{2b} &= \epsilon^{\mu}(k) \left[\frac{(-ig_s)(i)\bar{n}_{\mu}}{\bar{n} \cdot k + i\varepsilon} \ell_{\perp}^{\rho} \Delta_{\rho}^{\ell_{\perp}} (-\not{p}_{\perp}) + g_s \ell_{\perp}^{\rho} \Delta_{\rho}^{\ell_{\perp}} \gamma_{\perp\mu} \right] P_n \dots, \\ A_{2m} &= \epsilon^{\mu}(k) \frac{(-ig_s)(i)\bar{n}_{\mu}}{\bar{n} \cdot k + i\varepsilon} (-m) P_n \dots, \end{aligned} \quad (18)$$

respectively. Here, $\epsilon^{\mu}(k)$ is the polarization of a hard-collinear gluon with momentum k . Note that, in A_1 , A_{2a} , and A_{2m} , $p^+ = k^+$ and $p_{\perp} = k_{\perp}$, owing to the multipole expansion of the soft-quark field. In A_{2b} , $p^+ = k^+$, but p_{\perp} is set equal to k_{\perp} only after differentiation with respect to ℓ_{\perp} , in accordance with Eq. (17).

We can work out the Ward identities for these amplitudes by carrying out a gauge transformation on the gluon field, which, at the lowest order in g_s , simply shifts the gluon polarization vector $\epsilon^{\mu}(k)$ by an amount that is proportional to the gluon momentum k :

$$\epsilon^{\mu}(k) \rightarrow \epsilon^{\mu}(k) + \beta k^{\mu}. \quad (19)$$

We drop the constant of proportionality β in subsequent discussions. The gauge term k^{μ}

gives the following contributions to the amplitudes A_1 , A_{2a} , and A_{2m} in Eq. (18):

$$\begin{aligned} A_1^{\text{gauge}} &= g_s(-\not{p}_\perp + \not{k}_\perp)P_n \dots \\ &= 0, \end{aligned} \tag{20a}$$

$$\begin{aligned} A_{2a}^{\text{gauge}} &= g_s \left[\left(-n \cdot p - \frac{p_\perp^2}{\bar{n} \cdot p} \right) + \left(n \cdot k + \frac{\not{k}_\perp \not{p}_\perp}{\bar{n} \cdot p} \right) \right] \frac{\not{p}}{2} P_n \dots \\ &= -g_s n \cdot \ell \frac{\not{p}}{2} P_n \dots, \end{aligned} \tag{20b}$$

$$A_{2m}^{\text{gauge}} = g_s(-m)P_n \dots, \tag{20c}$$

where we have used $k_\perp = p_\perp$, which follows from the multipole expansion of the soft-quark field q_s , and $n \cdot k = n \cdot p - n \cdot \ell$. The gauge term k^μ gives the following contribution to the amplitude A_{2b} in Eq. (18):

$$\begin{aligned} A_{2b}^{\text{gauge}} &= g_s \left[\ell_\perp^\rho \Delta_\rho^{\ell_\perp}(-\not{p}_\perp) + \ell_\perp^\rho \Delta_\rho^{\ell_\perp} \not{k}_\perp \right] P_n \dots \\ &= g_s \left[\ell_\perp^\rho \Delta_\rho^{\ell_\perp}(-\not{\ell}_\perp) \right] P_n \dots \\ &= -g_s \not{\ell}_\perp P_n \dots, \end{aligned} \tag{20d}$$

where we have used $k_\perp = p_\perp - \ell_\perp$, owing to the insertion of the ℓ_\perp into the hard-collinear subdiagram, which follows from the identity in Eq. (16). Note that the contributions in which $\Delta_\rho^{\ell_\perp}$ acts on the ellipsis (the remainder of the diagram) cancel between the first and second terms after the first equality in Eq. (20d).

We see that the order- λ^1 Lagrangian in Eq. (13) gives a vanishing contribution to the Ward identities. That is, it is gauge invariant. However, each of the order- λ^2 Lagrangians in Eq. (13) produces a nonzero contribution to the Ward identity, *i.e.*, a violation of gauge invariance, and we find that

$$\begin{aligned} A_{2a}^{\text{gauge}} + A_{2b}^{\text{gauge}} + A_{2m}^{\text{gauge}} &= g_s \left(-n \cdot \ell \frac{\not{p}}{2} - \not{\ell}_\perp - m \right) P_n \dots \\ &= g_s(-\not{\ell} - m)P_n \dots, \end{aligned} \tag{21}$$

where we have used $\not{p}P_n = 0$. We note that the violations of gauge invariance are proportional to soft-quark free equation of motion. This suggests that we can obtain a gauge-invariant form of the Lagrangian by discarding terms that are proportional to the soft-quark

equation of motion. In Sec. V, we will see that this is the case.⁵

A complete factorization formula, including both the radiative jet (hard-collinear) function and the soft function, must be gauge invariant because it reproduces full QCD to a given accuracy in λ . Therefore, we expect gauge invariance to be restored if we consider the soft function in conjunction with the radiative jet function. As we have seen, the order- λ^2 contributions to the radiative jet function that violate gauge invariance are proportional to the inverse of the soft-quark propagator $-\not{\ell} - m$. At the lowest order in g_s , the soft function is just the soft-quark propagator. Hence, soft function is canceled by the gauge-invariance violating contributions. Consequently, as we can see from the result for the radiative jet functions in Secs. IV and VII, all of the poles in the ℓ^- complex plane are in the upper half plane. We can then close the ℓ^- contour of integration in the lower half plane to obtain a vanishing result for the gauge-invariance-violating contribution. As we have mentioned, in Sec. V, we will use the formal procedure of discarding Lagrangian terms that are proportional to the soft-quark equation of motion in order to implement gauge invariance in the radiative jet function at the integrand level. The phenomenon that we see here, namely, the vanishing of contributions that are proportional to the soft-quark equation of motion, demonstrates the correctness of the formal procedure in lowest-order perturbation theory.

C. Missing diagrams

The violations of gauge invariance that we have noted arise because certain diagrams that would be present in full QCD are missing from the hard-collinear function because they contain a soft-quark propagator. The diagram of this type that appears in order g_s is shown on the left side of Fig. 4. Note that, because we are considering diagrams that contain a soft-quark propagator, momentum conservation no longer requires that the order- g_s^0 factors from the crossed circles appear in conjunction with hard-collinear gluons that attach to the Wilson line.

The amplitudes for the diagram in Fig. 4 that correspond to the crossed vertices from

⁵ Subtractions of terms that are proportional to the soft-quark equation of motion are used to derive the Lagrangian in Ref. [8].

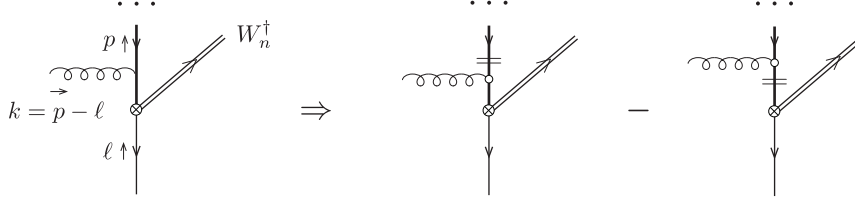


FIG. 4. Left side: the Feynman diagram in order g_s that is missing from the hard-collinear function. Right side: the corresponding Ward-identity contribution. The crossed vertex derives from the operators in Eq. (13).

$\mathcal{L}_1^{\text{BCDF}}$, $\mathcal{L}_{2a}^{\text{BCDF}}$, $\mathcal{L}_{2b}^{\text{BCDF}}$, and $\mathcal{L}_{2m}^{\text{BCDF}}$ are

$$A_{1,\text{miss}} = 0, \quad (22a)$$

$$A_{2a,\text{miss}} = \epsilon^\mu(k)(-n \cdot \ell) \frac{\not{n}}{2} P_n \frac{i}{-\ell - m + i\varepsilon} (ig_s) \gamma_\mu \dots, \quad (22b)$$

$$A_{2b,\text{miss}} = \epsilon^\mu(k) \ell_\perp^\rho \Delta_\rho^{\ell_\perp}(-\ell_\perp) P_n \frac{i}{-\ell - m + i\varepsilon} (ig_s) \gamma_\mu \dots, \quad (22c)$$

$$A_{2m,\text{miss}} = \epsilon^\mu(k)(-m) P_n \frac{i}{-\ell - m + i\varepsilon} (ig_s) \gamma_\mu \dots, \quad (22d)$$

respectively. Here, in keeping with the multipole expansion of the soft-quark field q_s in the Lagrangians in Eq. (13), we have discarded terms in the hard-collinear part that are proportional to ℓ_\perp , except in $A_{2b,\text{miss}}$. In the case of $A_{2b,\text{miss}}$, we set ℓ_\perp to zero only after the derivative in $\Delta_\rho^{\ell_\perp}$ has been taken. After we carry out the gauge transformation in Eq. (19), we obtain the following contributions of the gauge term k^μ to Eqs. (22a):

$$A_{1,\text{miss}}^{\text{gauge}} = 0, \quad (23a)$$

$$\begin{aligned} A_{2a,\text{miss}}^{\text{gauge}} &= -n \cdot \ell \frac{\not{n}}{2} P_n \frac{i}{-\ell - m + i\varepsilon} (ig_s) \not{k} \dots \\ &= -g_s n \cdot \ell \frac{\not{n}}{2} P_n \frac{1}{-\ell - m + i\varepsilon} [(-\not{p} - m) - (-\ell - m)] \dots, \end{aligned} \quad (23b)$$

$$\begin{aligned} A_{2b,\text{miss}}^{\text{gauge}} &= \ell_\perp^\rho \Delta_\rho^{\ell_\perp}(-\ell_\perp) P_n \frac{i}{-\ell - m + i\varepsilon} (ig_s) \not{k} \dots \\ &= g_s \ell_\perp^\rho \Delta_\rho^{\ell_\perp}(-\ell_\perp) P_n \frac{1}{-\ell - m + i\varepsilon} [(-\not{p} - m) - (-\ell - m)] \dots, \end{aligned} \quad (23c)$$

$$\begin{aligned} A_{2m,\text{miss}}^{\text{gauge}} &= (-m) P_n \frac{i}{-\ell - m + i\varepsilon} (ig_s) \not{k} \dots \\ &= g_s (-m) P_n \frac{1}{-\ell - m + i\varepsilon} [(-\not{p} - m) - (-\ell - m)] \dots, \end{aligned} \quad (23d)$$

which are represented by the diagram on the right side of Fig. 4. If the quark line with momentum $-p$ is an external line, then the first terms in the square brackets in each of the contributions above vanish on multiplying the quark spinor. Otherwise, they cancel contributions that arise from the gauge transformations for the sum over all attachments of the gluon with momentum k to other parts of the radiative jet function (the ellipses in Figs. 1 and 4).⁶ The second term in the square brackets in each of the contributions above cancels the corresponding gauge terms in Eqs. (20b), (20c), and (20d). This cancellation confirms our assertion that the violations of gauge invariance arise because of missing diagrams involving soft-quark propagators. Note that the contribution in Eq. (23a) that arises from the order- λ^1 Lagrangian vanishes, in keeping with the gauge invariance of that Lagrangian.

IV. RADIATIVE JET FUNCTION IN ORDER α_s FROM THE BCDF LAGRANGIANS

Now let us test the gauge invariance of radiative jet functions that are derived from the BCDF Lagrangians. From the BCDF Lagrangians at $O(\lambda^2)$ in Eq. (13), we can construct the following radiative jet functions:

$$\begin{aligned}
A(\ell^-) &= \int d^D x e^{-i\frac{\ell^- x^+}{2}} \\
&\quad \times \langle \mathcal{Q}\bar{\mathcal{Q}}(^3S_1^{[1]}, p, p) | T \left[W_n^\dagger \left(in \cdot D_n + i\not{D}_{n\perp} \frac{1}{i\bar{n} \cdot D_n} i\not{D}_{n\perp} \right) \frac{\not{n}}{2} \xi_n \right]^{\beta, b} (x) (\bar{\xi}_n W_n)^{\alpha, a}(0) | 0 \rangle, \\
B_\rho(\ell^-) &= \int d^{D-2} \ell_\perp \frac{\partial}{\partial \ell_\perp^\rho} [\delta^{D-2}(\ell_\perp)] \\
&\quad \times \int d^D x e^{-i\frac{\ell^- x^+}{2}} e^{-i\ell_\perp \cdot x_\perp} \langle \mathcal{Q}\bar{\mathcal{Q}}(^3S_1^{[1]}, p, p) | T (W_n^\dagger i\not{D}_{n\perp} \xi_n)^{\beta, b} (x) (\bar{\xi}_n W_n)^{\alpha, a}(0) | 0 \rangle, \\
M(\ell^-) &= \int d^D x e^{-i\frac{\ell^- x^+}{2}} \langle \mathcal{Q}\bar{\mathcal{Q}}(^3S_1^{[1]}, p, p) | T (-mW_n^\dagger \xi_n)^{\beta, b} (x) (\bar{\xi}_n W_n)^{\alpha, a}(0) | 0 \rangle, \tag{24}
\end{aligned}$$

where α, β and a, b are Dirac and color indices, respectively. In these expressions, the first factors of the SCET operators arise from the BCDF Lagrangians $\mathcal{L}_{2a}^{\text{BCDF}}$, $\mathcal{L}_{2b}^{\text{BCDF}}$, and $\mathcal{L}_{2m}^{\text{BCDF}}$ in Eq. (13), respectively, while the second factors of the SCET operators, namely, $\bar{\xi}_n W_n$, arise from the hard-collinear part of the hard-to-hard-collinear transition operator in the amplitude for a hard-scattering process. The couplings of minus-polarized soft-gluon fields

⁶ This can be seen by direct application of the Ward identities for the elementary QCD vertices and the Wilson line W_n that appears in the radiative jet function.

to hard-collinear fields have been removed by making use of the BPS field redefinitions [Eq. (14)]. This has the effect of replacing D in $A(\ell^-)$ with D_n . We have taken the vacuum to $Q\bar{Q}$ matrix elements of these operators, where Q and \bar{Q} are massive, on-shell quark states. These matrix elements are convenient because, for them, the difficulty with gauge invariance appears at the Born level, rather than at the loop level. For definiteness, we take the Q and the \bar{Q} to be in a spin-triplet, color-singlet state with zero relative momentum between the Q and the \bar{Q} . (This is an S -wave state.) Then, we can take both the Q and the \bar{Q} to have momentum p . We can, without loss of generality, choose a frame in which $p_\perp = 0$. Note that, because the momentum p is on the mass shell, it satisfies collinear scaling, rather than hard-collinear scaling:

$$\begin{aligned} p^+ &\sim Q\lambda^0, \\ p_\perp &= 0, \\ p^- &= m^2/p^+ \sim Q\lambda^4. \end{aligned} \tag{25}$$

Note also that the Ward-identity arguments of Sec. III, which were presented for the case of hard-collinear scaling, are also valid for the case of collinear scaling.

We realize the $Q\bar{Q}$ color and spin states through the application of the standard spin and color projection operators, whose product is given by

$$\Pi_{3S_1^{[1]}}^{cd} = -\frac{\not{\epsilon}^*(\not{p} + m)}{2\sqrt{2}m} \times \frac{\delta^{cd}}{\sqrt{N_c}}, \tag{26}$$

where ϵ^* is the polarization vector of the external $3S_1^{[1]}$ state, which satisfies $\epsilon^* \cdot p = 0$.

The $O(\alpha_s)$ diagrams for the radiative jet functions are given in Fig. 5. Note that the gluon must connect the soft-quark side of the diagram, which is to the left of the $Q\bar{Q}$ state, to the hard-quark side of the diagram, which is to the right of the $Q\bar{Q}$ state, in order for hard-collinear-momentum conservation to be satisfied. The left two diagrams involve the Feynman rule $V_i^{(0)}$ (Figs. 2 and 3) on their soft-quark sides, and the right two diagrams involve the Feynman rule $V_i^{(1)}$ (Figs. 2 and 3) on their soft-quark sides with $i = 2a, 2b, 2m$.

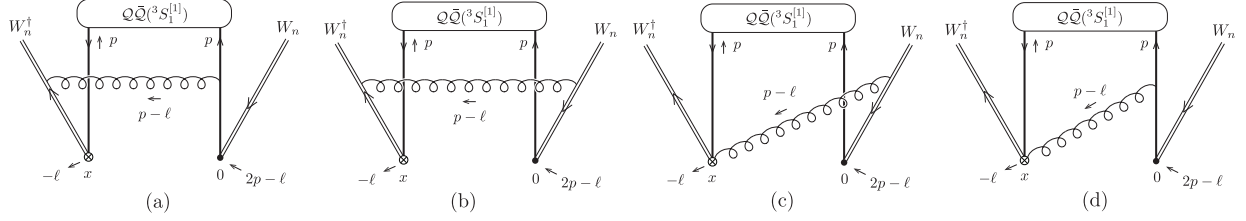


FIG. 5. The LO diagrams for the radiative jet functions. Note that the soft momentum ℓ^μ flows in through the vertex on the soft-quark side at x and flows out through the vertex on the hard-quark side at 0 . The Feynman rules for the crossed circle vertex are given in Figs. 2 and 3.

A. Feynman gauge

First, let us consider the computations of the radiative jet functions in the Feynman gauge.

For the A radiative jet function, only the diagram of Fig. 5(c) contributes. The diagram of Fig. 5(b) vanishes because the Wilson-line vertices give $\bar{n} \cdot \bar{n} = 0$. The diagrams of Figs. 5(a) and (d) are power suppressed, as we show in Appendix B.

For the B radiative jet function, only the diagram of Fig. 5(d) contributes. The diagram of Fig. 5(b) vanishes because the Wilson-line vertices give $\bar{n} \cdot \bar{n} = 0$. The diagram of Fig. 5(c) vanishes because the crossed vertex gives $\bar{n} \cdot \gamma_\perp = 0$. The diagram of Fig. 5(a) is power suppressed because of the scaling in Eq. (25).

For the M radiative jet function, only the diagram of Fig. 5(a) contributes. The diagram of Fig. 5(b) vanishes because the Wilson-line vertices give $\bar{n} \cdot \bar{n} = 0$, and the diagrams of Figs. 5(c) and (d) do not contribute because $V_{2m}^{(1)} = 0$ (Fig. 2).

Then, a straightforward calculation in the Feynman gauge yields the following Born-level

radiative jet functions:

$$\begin{aligned}
A_{(c),\text{Feynman}}(\ell^-) &= (T^e)^{bc}(T^e)^{da} \left\{ g_s \left(n_\mu + \gamma_{\perp\mu} \frac{\not{p}_\perp}{\bar{n} \cdot p} \right) \frac{\not{\eta}}{2} P_n \Pi_{3S_1^{[1]}}^{cd} P_{\bar{n}} \right\}^{\beta\alpha} \frac{i(i g_s \bar{n}^\mu)}{-\bar{n} \cdot (p - \ell) + i\varepsilon} \frac{-i}{(p - \ell)^2 + i\varepsilon} \\
&= -\frac{i g_s^2 C_F \delta^{ba}}{\sqrt{2N_c} m p^+} \frac{1}{(-\ell^- + i\varepsilon)} \left(\frac{\not{\eta} \not{\eta} \not{\epsilon}^*}{4} \right)^{\beta\alpha}, \\
B_{\rho(d),\text{Feynman}}(\ell^-) &= \int d^{D-2} \ell_\perp \frac{\partial}{\partial \ell_\perp^\rho} [\delta^{D-2}(\ell_\perp)] (T^e)^{bc}(T^e)^{da} \\
&\quad \times \left\{ (g_s \gamma_{\perp\mu}) P_n \Pi_{3S_1^{[1]}}^{cd} (i g_s \gamma^\mu) \frac{i}{2\not{p} - \not{\ell} - m + i\varepsilon} P_{\bar{n}} \right\}^{\beta\alpha} \frac{-i}{(p - \ell)^2 + i\varepsilon} \\
&= 0, \\
M_{(a),\text{Feynman}}(\ell^-) &= (T^e)^{bc}(T^e)^{da} \left\{ (-m) P_n \Pi_{3S_1^{[1]}}^{cd} (i g_s \gamma_\mu) \frac{i}{2\not{p} - \not{\ell} - m + i\varepsilon} P_{\bar{n}} \right\}^{\beta\alpha} \frac{i(-i g_s \bar{n}_\nu)}{\bar{n} \cdot (p - \ell) + i\varepsilon} \\
&\quad \times \frac{-i g^{\mu\nu}}{(p - \ell)^2 + i\varepsilon} \\
&= -\frac{i g_s^2 C_F \delta^{ba}}{\sqrt{2N_c} p^+} \frac{1}{(-\ell^- + i\varepsilon)^2} \left(\frac{\not{\eta} \not{\epsilon}^*}{2} \right)^{\beta\alpha}, \tag{27}
\end{aligned}$$

where we have kept only the leading nonzero power in λ in the last lines of these expressions.

In the case of $B_{\rho(d),\text{Feynman}}(\ell^-)$, we have used

$$[\gamma_\mu^\perp P_n \not{\epsilon}^*(\not{p} + m) \gamma^\mu (2\not{p} - \not{\ell} + m) P_{\bar{n}}]^{\beta\alpha} = 0, \tag{28}$$

which is valid through the power in λ in which we are interested.

B. Light-cone gauge

Next, let us consider the radiative jet functions in the light-cone gauge, which is defined by the gauge condition

$$\bar{n} \cdot G_n \Big|_{\text{light-cone gauge}} = 0, \tag{29}$$

from which it follows that the gluon-propagator polarization sum is

$$-g^{\mu\nu} + \frac{k^\mu \bar{n}^\nu + \bar{n}^\mu k^\nu}{k \cdot \bar{n}}. \tag{30}$$

Here, k is the gluon momentum. In the light-cone gauge, the n -hard-collinear Wilson line [defined in Eq. (11)] becomes unity, and so the diagrams involving Wilson lines vanish. (Equivalently, one can see that the polarization sum in Eq. (30) vanishes on contraction with the Wilson-line vertex $-ig\bar{n}_\mu$.) Consequently, in the light-cone gauge, only the diagram of Fig. 5(d) can contribute.

The calculation of the contribution of the diagram of Fig. 5(d) in the light-cone gauge is straightforward. We obtain

$$\begin{aligned}
A_{(d),\text{light-cone}}(\ell^-) &= (T^e)^{bc}(T^e)^{da} \left\{ g_s \left(n_\mu + \gamma_{\perp\mu} \frac{\not{p}_\perp}{\bar{n} \cdot p} \right) P_n \Pi_{3S_1^{[1]}}^{cd}(ig_s \gamma_\nu) \frac{i}{2\not{p} - \not{\ell} - m + i\varepsilon} P_{\bar{n}} \right\}^{\beta\alpha} \\
&\quad \times \frac{i}{(p-\ell)^2 + i\varepsilon} \left[-g^{\mu\nu} + \frac{(p-\ell)^\mu \bar{n}^\nu + \bar{n}^\mu (p-\ell)^\nu}{(p-\ell) \cdot \bar{n}} \right] \\
&= -\frac{2ig_s^2 C_F \delta^{ba}}{\sqrt{2N_c} mp^+} \frac{1}{(-\ell^- + i\varepsilon)} \left(\frac{\not{\ell}_\perp \not{\ell}^*}{4} \right)^{\beta\alpha}, \\
B_{\rho(d),\text{light-cone}}(\ell^-) &= \int d^{D-2} \ell_\perp \partial_{\ell_\perp \rho} [\delta^{D-2}(\ell_\perp)] (T^e)^{bc}(T^e)^{da} \left\{ (g_s \gamma_\mu^\perp) P_n \Pi_{3S_1^{[1]}}^{cd}(ig_s \gamma_\nu) \frac{i}{2\not{p} - \not{\ell} - m + i\varepsilon} P_{\bar{n}} \right\}^{\beta\alpha} \\
&\quad \times \frac{i}{(p-\ell)^2 + i\varepsilon} \left[-g^{\mu\nu} + \frac{(p-\ell)^\mu \bar{n}^\nu + \bar{n}^\mu (p-\ell)^\nu}{(p-\ell) \cdot \bar{n}} \right] \\
&= \int d^{D-2} \ell_\perp \partial_{\ell_\perp \rho} [\delta^{D-2}(\ell_\perp)] \frac{ig_s^2 C_F \delta^{ba}}{\sqrt{2N_c} mp^+} \frac{1}{(-\ell^- + i\varepsilon)^2} \left(\frac{\not{\ell}_\perp \not{\ell}^*}{2} \right)^{\beta\alpha} \\
&= -\frac{ig_s^2 C_F \delta^{ba}}{\sqrt{2N_c} mp^+} \frac{1}{(-\ell^- + i\varepsilon)^2} \left(\frac{\gamma_{\perp\rho} \not{\ell}^*}{2} \right)^{\beta\alpha}, \\
M_{(d),\text{light-cone}}(\ell^-) &= 0, \tag{31}
\end{aligned}$$

where we have kept only the leading nonzero power of λ in the last line of each expression. Note that $M_{(d),\text{light-cone}}(\ell^-) = 0$ because $V_{2m}^{(1)} = 0$ in Fig. 2. By comparing the light-cone-gauge results in Eq. (31) with the Feynman-gauge results in Eq. (27), we conclude that all three radiative jet functions in Eq. (24) are not gauge invariant. The difference between the light-cone-gauge and the Feynman-gauge calculations is

$$\begin{aligned}
& [A_{(d),\text{light-cone}}(\ell^-) + (-\ell_\perp^\rho) B_{\rho(d),\text{light-cone}}(\ell^-) + M_{(d),\text{light-cone}}(\ell^-)] \\
& - [A_{(c),\text{Feynman}}(\ell^-) + (-\ell_\perp^\rho) B_{\rho(d),\text{Feynman}}(\ell^-) + M_{(a),\text{Feynman}}(\ell^-)] \\
& = -\frac{ig_s^2 C_F \delta^{ba}}{\sqrt{2N_c} mp^+} \frac{1}{(-\ell^- + i\varepsilon)^2} \left[(-\not{\ell} - m) \frac{\not{\ell}^*}{2} \right]^{\beta\alpha}, \tag{32}
\end{aligned}$$

where we have contracted $(-\ell_\perp^\rho)$ into B_ρ since an additional factor of $(-\ell_\perp^\rho)$ is present in the soft function that is associated with B_ρ , relative to the soft functions that are associated with A and M . In the last line of Eq. (32), we have inserted $-\ell^+ \frac{\not{\ell}}{2} \not{\ell} = 0$ in order to obtain the factor $-\not{\ell} - m$. As is expected from our Ward-identity analysis, the gauge-variant terms are proportional to the inverse of the soft-quark propagator.

C. Covariant gauge

We can also consider the radiative jet functions in a general covariant gauge, in which the gluon polarization sum is given by

$$-g^{\mu\nu} + \alpha \frac{k^\mu k^\nu}{k^2}, \quad (33)$$

where α is the gauge parameter.

In order α_s in a general covariant gauge, the sum over all connections of the gluon to the quark line and the W_n Wilson line (on the right side of a radiative-jet diagrams) is gauge invariant, independently of the rest of the diagram. Hence, the term in the polarization sum that is proportional to α vanishes in the sum over all connections of the gluon to the quark line and the W_n Wilson line, and one obtains the Feynman-gauge result.

However, in order α_s^2 the situation is more complicated. We have checked that, in the Abelian case, there is a remnant from the terms that are proportional to α in the polarization sum that is nonzero at the integrand level. This suggests that a gauge dependence exists in general covariant gauges in order α_s^2 .

V. GAUGE INVARIANT SCET LAGRANGIANS

In this section, we modify the BCDF Lagrangians to obtain gauge-invariant Lagrangians that describe the coupling of a soft quark to a hard-collinear quark. In order to account for the gauge-violating contribution in Eq. (21), we introduce the following subtraction

Lagrangian:

$$\begin{aligned}
\Delta\mathcal{L}_2(x) &= \left[\bar{q}_s \left(-i\overleftarrow{\mathcal{D}}_s - m \right) \right] (x^+) (W_n^\dagger \xi_n)(x) \\
&= \left[\bar{q}_s \left(\frac{\not{n}}{2} in \cdot D_s - i\overleftarrow{\mathcal{D}}_{s\perp} - m \right) \right] (x^+) (W_n^\dagger \xi_n)(x),
\end{aligned} \tag{34}$$

where, in the second line, we have used $\not{n}\xi_n = \not{n}P_n\psi_n = 0$, and performed an integration by parts for the term that is proportional to $in \cdot D_s$. This integration by parts is valid because the minus component of the soft momentum flows into the hard-collinear parts of the Lagrangian. We remind the reader that the position arguments of the soft fields have been multipole expanded (depend only on the plus component of the coordinate), but only after the derivatives acting on the soft fields have been taken.

The modified Lagrangian that describes the coupling of a soft quark to a hard-collinear quark in order λ^2 is

$$\begin{aligned}
\mathcal{L}_2^{\text{mod}} &= \mathcal{L}_{2a}^{\text{BCDF}} + \mathcal{L}_{2b}^{\text{BCDF}} + \mathcal{L}_{2m}^{\text{BCDF}} - \Delta\mathcal{L}_2 \\
&= \bar{q}_s W_n^\dagger in \cdot D \frac{\not{n}}{2} \xi_n - \bar{q}_s in \cdot D_s W_n^\dagger \frac{\not{n}}{2} \xi_n + \bar{q}_s W_n^\dagger i\mathcal{D}_{n\perp} \frac{1}{in \cdot D_n} i\mathcal{D}_{n\perp} \frac{\not{n}}{2} \xi_n \\
&\quad + \bar{q}_s (-i\overleftarrow{\mathcal{D}}_{s\perp}) \cdot ix_\perp W_n^\dagger i\mathcal{D}_{n\perp} \xi_n - \bar{q}_s (-i\overleftarrow{\mathcal{D}}_{s\perp}) W_n^\dagger \xi_n,
\end{aligned} \tag{35}$$

where we omit the position arguments for simplicity. Note that the quark-mass-dependent Lagrangian $\mathcal{L}_{2m}^{\text{BCDF}}$ is canceled by the mass term of $\Delta\mathcal{L}_2$ in Eq. (34), and so the $O(\lambda^2)$ interactions between a soft quark and a hard-collinear quark are independent of the quark mass.

At this stage, longitudinally polarized soft gluons can still interact with the hard-collinear subdiagram. As we have mentioned previously, such interactions can be factored into Wilson lines by making use of the BPS field redefinitions [4], which are shown in Eq. (14). Using the BPS field redefinitions and the identities

$$S_n^\dagger in \cdot D_s S_n = in \cdot \partial, \tag{36a}$$

$$S_n^\dagger in \cdot D' S_n = S_n^\dagger n \cdot (S_n g_s G_n S_n^\dagger + iD_s) S_n = in \cdot D_n, \tag{36b}$$

$$\begin{aligned}
V_{2a}^{\text{mod}(0)} &= \left(-n \cdot k - \frac{p_\perp^2}{\bar{n} \cdot p} \right) \frac{\not{n}}{2} \\
V_{2b}^{\text{mod}(0)} &= \ell_\perp^\rho \left(\Delta_\rho^{\ell_\perp}(-\not{p}_\perp) + \gamma_{\perp\rho} \right) \\
V_{2a}^{\text{mod}(1)} &= g_s T^A \left(n_\mu + \gamma_{\perp\mu} \frac{\not{p}_\perp}{\bar{n} \cdot p} \right) \frac{\not{n}}{2} \\
V_{2b}^{\text{mod}(1)} &= g_s T^A \ell_\perp^\rho \Delta_\rho^{\ell_\perp} \gamma_{\perp\mu}
\end{aligned}$$

FIG. 6. The Feynman rules for the crossed circles in Fig. 1 for the Lagrangians in Eq. (38). V_{2a}^{mod} and V_{2b}^{mod} represent the crossed-circle contributions that arise from $\mathcal{L}_{2a}^{\text{mod,BPS}}$ and $\mathcal{L}_{2b}^{\text{mod,BPS}}$, respectively. The superscripts (0) and (1) denote the order- g_s^0 and order- g_s^1 contributions of the crossed circle, respectively.

we rewrite Eq. (35) as follows:

$$\mathcal{L}_2^{\text{mod,BPS}} = \mathcal{L}_{2a}^{\text{mod,BPS}} + \mathcal{L}_{2b}^{\text{mod,BPS}}, \quad (37)$$

where

$$\mathcal{L}_{2a}^{\text{mod,BPS}} = \bar{q}_s S_n \left[W_n^\dagger \left(-in \cdot \overleftarrow{D}_n \right) + W_n^\dagger i \not{D}_{n\perp} \frac{1}{i\bar{n} \cdot D_n} i \not{D}_{n\perp} \right] \frac{\not{n}}{2} \xi_n, \quad (38a)$$

$$\mathcal{L}_{2b}^{\text{mod,BPS}} = \bar{q}_s (-i \overleftarrow{D}_{s\perp}^\rho) S_n \left(ix_{\perp\rho} W_n^\dagger i \not{D}_{n\perp} \xi_n - \gamma_{\perp\rho} W_n^\dagger \xi_n \right). \quad (38b)$$

Here, in the first term of $\mathcal{L}_{2a}^{\text{mod,BPS}}$, the covariant derivative $(-in \cdot \overleftarrow{D}_n)$ should be understood as acting only on the Wilson line W_n^\dagger . The Feynman rules for these modified Lagrangians are given in Fig. 6. Again, we note that, owing to the use of the multipole expansion, the soft transverse momentum ℓ_\perp should be set to zero, except in the terms involving the operator $\Delta_\rho^{\ell_\perp}$ [Eq. (17)]. For those terms, ℓ_\perp is set to zero after differentiation with respect to ℓ_\perp .

A. Gauge invariance and Ward identities of the modified Lagrangians

Let us repeat the gauge-invariance analysis of Sec. IIIB for the modified $O(\lambda^2)$ SCET Lagrangians in Eq. (38). The amplitudes for $\mathcal{L}_{2a}^{\text{mod,BPS}}$ and $\mathcal{L}_{2b}^{\text{mod,BPS}}$, which correspond to

the diagram in Fig. 1, are

$$A_{2a}^{\text{mod}} = \epsilon^\mu(k) \left[\frac{(-ig_s)(i)\bar{n}_\mu}{\bar{n} \cdot k + i\varepsilon} \left(-n \cdot k - \frac{p_\perp^2}{\bar{n} \cdot p} \right) + g_s \left(n_\mu + \gamma_{\perp\mu} \frac{\not{p}_\perp}{\bar{n} \cdot p} \right) \right] \frac{\not{n}}{2} P_n \dots, \quad (39a)$$

$$A_{2b}^{\text{mod}} = \epsilon^\mu(k) \left[\frac{(-ig_s)(i)\bar{n}_\mu}{\bar{n} \cdot k + i\varepsilon} \ell_\perp^\rho \left(\Delta_\rho^{\ell_\perp}(-\not{p}_\perp) + \gamma_{\perp\rho} \right) + g_s \ell_\perp^\rho \Delta_\rho^{\ell_\perp} \gamma_{\perp\mu} \right] P_n \dots, \quad (39b)$$

respectively. We obtain the Ward identities for these amplitudes by replacing the polarization vector $\epsilon^\mu(k)$ with the factor k^μ from the gauge transformation in Eq. (19). The results are as follows:

$$A_{2a}^{\text{mod,gauge}} = g_s \left[\left(-n \cdot k - \frac{p_\perp^2}{\bar{n} \cdot p} \right) + \left(n \cdot k + \frac{\not{k}_\perp \not{p}_\perp}{\bar{n} \cdot p} \right) \right] \frac{\not{n}}{2} P_n \dots \quad (40a)$$

$$= 0,$$

$$A_{2b}^{\text{mod,gauge}} = g_s \left[\ell_\perp^\rho \left(\Delta_\rho^{\ell_\perp}(-\not{p}_\perp) + \gamma_{\perp\rho} \right) + \ell_\perp^\rho \Delta_\rho^{\ell_\perp} \not{k}_\perp \right] P_n \dots \quad (40b)$$

$$= 0,$$

where we have used $k_\perp = p_\perp$ for $A_{2a}^{\text{mod,gauge}}$, owing to the multipole expansion of the soft-quark field, and $k_\perp = p_\perp - \ell_\perp$ for $A_{2b}^{\text{mod,gauge}}$, owing to the insertion of ℓ_\perp that follows from the identity in Eq. (16). Note that the contributions in which $\Delta_\rho^{\ell_\perp}$ acts on the ellipsis (the remainder of the diagram) cancel between the first and third terms after the first equality in Eq. (40b). We conclude that the modified Lagrangians in Eq. (38) are separately gauge invariant.

B. Missing diagrams for the modified Lagrangians

Now let us consider the contributions of the modified Lagrangians to the missing diagram in Fig. 4. The amplitudes for the diagram in Fig. 4 that correspond to the crossed vertices from $\mathcal{L}_{2a}^{\text{mod,BPS}}$ and $\mathcal{L}_{2b}^{\text{mod,BPS}}$ are

$$A_{2a,\text{miss}}^{\text{mod}} = 0, \quad (41a)$$

$$A_{2b,\text{miss}}^{\text{mod}} = \epsilon^\mu(k) \ell_\perp^\rho \left(\Delta_\rho^{\ell_\perp}(-\not{\ell}_\perp) + \gamma_{\perp\rho} \right) P_n \frac{i}{-\not{\ell} - m + i\varepsilon} (ig_s) \gamma_\mu \dots \quad (41b)$$

$$= 0,$$

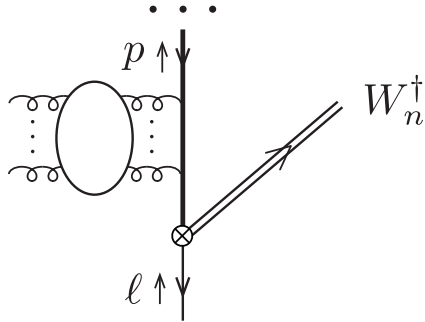


FIG. 7. The general form of the missing diagrams at all orders in g_s . The blob includes gluon self interactions and ghost loops.

respectively. Here, for $A_{2a,\text{miss}}^{\text{mod}}$, we have performed the multipole expansion to set ℓ_\perp to 0, and for $A_{2b,\text{miss}}^{\text{mod}}$, we have used

$$\ell_\perp^\rho (\Delta_\rho^{\ell_\perp}(-\ell_\perp) + \gamma_{\perp\rho}) = (\ell_\perp^\rho \Delta_\rho^{\ell_\perp}(-\ell_\perp) + \ell_\perp) = 0. \quad (42)$$

We see that the modified Lagrangians in Eq. (38) give vanishing contributions in order g_s to the missing diagram in Fig. 4 and are, therefore, gauge invariant to this order.

VI. GAUGE INVARIANCE TO ALL ORDERS IN g_s

We now argue that the gauge invariances of order- λ^1 Lagrangian in Eq. (13a) and the modified order- λ^2 Lagrangians in Eq. (38) hold to all orders in g_s . First, we note that the all-orders missing diagrams have exactly one soft-quark propagator and that all collinear gluon attachments are to the collinear-subdiagram side of the soft-quark propagator. These diagrams are of the form that is shown in Fig. 7. A crucial feature of these diagrams is that the crossed-vertex factors are independent of the hard-collinear gluon attachments. That is, they are equal to the lowest-order crossed-vertex factors. Furthermore, we have seen in Eqs. (22a) and (41) that each crossed-vertex factor gives a vanishing result when no hard-collinear momentum flows through the crossed vertex. Therefore, the missing diagrams give vanishing contributions, ensuring the gauge invariance of the Lagrangians in Eqs. (13a) and (38).

VII. RADIATIVE JET FUNCTION IN ORDER α_s FROM THE MODIFIED LAGRANGIANS

In this section, we consider radiative jet functions that arise from the gauge-invariant Lagrangians in Eq. (38). Using the two $O(\lambda^2)$ gauge-invariant Lagrangians, we construct the following radiative jet functions:

$$\begin{aligned}
A^{\text{mod}}(\ell^-) &= \int d^D x e^{-i\frac{\ell^- x^+}{2}} \langle \mathcal{Q}\bar{\mathcal{Q}}(^3S_1^{[1]}, p, p) | \\
&\quad \times T \left\{ \left[W_n^\dagger \left(-in \cdot \overleftarrow{D}_n \right) + W_n^\dagger i \not{D}_{n\perp} \frac{1}{i\bar{n} \cdot D_n} i \not{D}_{n\perp} \right] \frac{\not{n}}{2} \xi_n \right\}^{\beta, b} (x) (\bar{\xi}_n W_n)^{\alpha, a}(0) | 0 \rangle, \\
B_{1\rho}^{\text{mod}}(\ell^-) &= \int d^{D-2} \ell_\perp \frac{\partial}{\partial \ell_\perp^\rho} [\delta^{D-2}(\ell_\perp)] \\
&\quad \times \int d^D x e^{-i\frac{\ell^- x^+}{2}} e^{-i\ell_\perp \cdot x_\perp} \langle \mathcal{Q}\bar{\mathcal{Q}}(^3S_1^{[1]}, p, p) | T (W_n^\dagger i \not{D}_{n\perp} \xi_n)^{\beta, b} (x) (\bar{\xi}_n W_n)^{\alpha, a}(0) | 0 \rangle, \\
B_{2\rho}^{\text{mod}}(\ell^-) &= \int d^D x e^{-i\frac{\ell^- x^+}{2}} \langle \mathcal{Q}\bar{\mathcal{Q}}(^3S_1^{[1]}, p, p) | T (-\gamma_{\perp\rho} W_n^\dagger \xi_n)^{\beta, b} (x) (\bar{\xi}_n W_n)^{\alpha, a}(0) | 0 \rangle. \tag{43}
\end{aligned}$$

Here, we have split the contribution from $\mathcal{L}_{2b}^{\text{mod, BPS}}$ in Eq. (38) into the contributions $B_{1\rho}^{\text{mod}}$ and $B_{2\rho}^{\text{mod}}$ because these contributions contain different prescriptions for the multipole expansion of the soft momentum ℓ . In accordance with our Ward-identity result in Eq. (40b), we will find that only the sum of $B_{1\rho}^{\text{mod}}$ and $B_{2\rho}^{\text{mod}}$ is gauge invariant.

In the Feynman gauge, we find that the diagrams of Figs. 5(a) and (c) contribute to the A^{mod} radiative jet function. (When we use the modified Feynman rules in Fig. 6, diagram (a) is no longer power suppressed.) We also find that the sole contribution to the $B_{1\rho}^{\text{mod}}$ radiative jet function arises from the diagram of Fig. 5(d), and the sole contribution to the $B_{2\rho}^{\text{mod}}$ radiative jet function arises from the diagram of Fig. 5(a). (The reasoning is the same as for the B and M radiative jet functions in Sec. IV A.) By making use of the Feynman

rules in Fig. 6, we obtain

$$\begin{aligned}
A_{(a),\text{Feynman}}^{\text{mod}}(\ell^-) &= (T^e)^{bc}(T^e)^{da} \left\{ \left[-n \cdot (p - \ell) \frac{\not{n}}{2} \right] P_n \Pi_{3S_1^{[1]}}^{cd}(ig_s \gamma_\mu) \frac{i}{2\not{p} - \not{\ell} - m + i\varepsilon} P_{\bar{n}} \right\}^{\beta\alpha} \\
&\quad \times \frac{i(-ig_s \bar{n}^\mu)}{\bar{n} \cdot (p - \ell) + i\varepsilon} \frac{-i}{(p - \ell)^2 + i\varepsilon} \\
&= -\frac{ig_s^2 C_F \delta^{ba}}{\sqrt{2N_c} mp^+} \frac{1}{(-\ell^- + i\varepsilon)} \left(\frac{\not{n} \not{\ell} \not{\ell}^*}{4} \right)^{\beta\alpha}, \\
A_{(c),\text{Feynman}}^{\text{mod}}(\ell^-) &= A_{(c),\text{Feynman}}(\ell^-) \\
&= -\frac{ig_s^2 C_F \delta^{ba}}{\sqrt{2N_c} mp^+} \frac{1}{(-\ell^- + i\varepsilon)} \left(\frac{\not{n} \not{\ell} \not{\ell}^*}{4} \right)^{\beta\alpha}, \\
B_{1\rho,(d),\text{Feynman}}^{\text{mod}}(\ell^-) &= B_{\rho(d),\text{Feynman}}(\ell^-) \\
&= 0, \\
B_{2\rho,(a),\text{Feynman}}^{\text{mod}}(\ell^-) &= (T^e)^{bc}(T^e)^{da} \left\{ (-\gamma_{\perp\rho}) P_n \Pi_{3S_1^{[1]}}^{cd}(ig_s \gamma_\mu) \frac{i}{2\not{p} - \not{\ell} - m + i\varepsilon} P_{\bar{n}} \right\}^{\beta\alpha} \\
&\quad \times \frac{i(-ig_s \bar{n}_\nu)}{\bar{n} \cdot (p - \ell) + i\varepsilon} \frac{-ig^{\mu\nu}}{(p - \ell)^2 + i\varepsilon} \\
&= -\frac{ig_s^2 C_F \delta^{ba}}{\sqrt{2N_c} mp^+} \frac{1}{(-\ell^- + i\varepsilon)^2} \left(\frac{\gamma_{\perp\rho} \not{\ell} \not{\ell}^*}{2} \right)^{\beta\alpha}. \tag{44}
\end{aligned}$$

We note that $A_{(c),\text{Feynman}}^{\text{mod}}(\ell^-) = A_{(c),\text{Feynman}}(\ell^-)$ and $B_{1\rho,(d),\text{Feynman}}^{\text{mod}}(\ell^-) = B_{1\rho,(d),\text{Feynman}}(\ell^-)$, which follows from $V_{2a}^{\text{mod}(1)} = V_{2a}^{(1)}$ and $V_{2b}^{\text{mod}(1)} = V_{2b}^{(1)}$ (Figs. 2, 3, and 6).

In the light-cone gauge, only the diagram of Fig. 5(d) contributes to the radiative jet function. We find that

$$\begin{aligned}
A_{(d),\text{light-cone}}^{\text{mod}}(\ell^-) &= A_{(d),\text{light-cone}}(\ell^-) \\
&= -\frac{2ig_s^2 C_F \delta^{ba}}{\sqrt{2N_c} mp^+} \frac{1}{(-\ell^- + i\varepsilon)} \left(\frac{\not{n} \not{\ell} \not{\ell}^*}{4} \right)^{\beta\alpha}, \\
B_{1\rho,(d),\text{light-cone}}^{\text{mod}}(\ell^-) &= B_{\rho(d),\text{light-cone}}(\ell^-) \\
&= -\frac{ig_s^2 C_F \delta^{ba}}{\sqrt{2N_c} mp^+} \frac{1}{(-\ell^- + i\varepsilon)^2} \left(\frac{\gamma_{\perp\rho} \not{\ell} \not{\ell}^*}{2} \right)^{\delta\alpha}, \\
B_{2\rho,(d),\text{light-cone}}^{\text{mod}}(\ell^-) &= 0, \tag{45}
\end{aligned}$$

where we have used the results in Eq. (31), since $V_{2a}^{\text{mod}(1)} = V_{2a}^{(1)}$ and $V_{2b}^{\text{mod}(1)} = V_{2b}^{(1)}$ (Figs. 2, 3, and 6). Note that $B_{2\rho,(d),\text{light-cone}}^{\text{mod}}(\ell^-) = 0$ because, as can be seen from Fig. 6, the relevant

order- g_s vertex vanishes.

We conclude that the radiative jet functions are identical in the Feynman gauge and the light-cone gauge:

$$\begin{aligned}
 A_{(a),\text{Feynman}}^{\text{mod}}(\ell^-) + A_{(c),\text{Feynman}}^{\text{mod}}(\ell^-) &= A_{(d),\text{light-cone}}^{\text{mod}}(\ell^-), \\
 B_{1\rho,(d),\text{Feynman}}^{\text{mod}}(\ell^-) + B_{2\rho,(a),\text{Feynman}}^{\text{mod}}(\ell^-) &= B_{1\rho,(d),\text{light-cone}}^{\text{mod}}(\ell^-) + B_{2\rho,(d),\text{light-cone}}^{\text{mod}}(\ell^-). \quad (46)
 \end{aligned}$$

As is expected from our Ward-identity analysis [Eq. (40)], A^{mod} is separately gauge invariant, while the sum of $B_{1\rho}^{\text{mod}}$ and $B_{2\rho}^{\text{mod}}$ is gauge invariant.

VIII. GAUGE INVARIANCE IN THE LABEL-MOMENTUM FORMULATION OF SCET

Finally, we mention that certain versions of the label-momentum formulation of SCET [8, 9] also contain expressions for the interactions between a soft-quark and a hard-collinear quark that are constructed from ostensibly gauge-invariant operators. The final expressions for the soft-quark-to-hard-collinear-quark Lagrangians are given in Eqs. (33) and (35) of Ref. [8] and Eq. (27) of Ref. [9]. They are derived by making use of the soft-quark equation of motion, which, as we have seen, is a crucial ingredient in deriving a gauge-invariant Lagrangian that describes the transitions of a soft quark to a hard-collinear quark.

The soft-quark-to-hard-collinear-quark Lagrangians in Eqs. (33) and (35) of Ref. [8] are proportional to the quantities \mathcal{M} and \mathcal{B}_{\perp}^c , and the soft-quark-to-hard-collinear-quark Lagrangians in Eq. (27) of Ref. [9] are proportional to the quantities $n \cdot M$ and \mathcal{B}_{\perp}^c . Since these quantities are commutators of covariant derivatives, the corresponding Lagrangians vanish when the gauge fields are set to zero. That is, these Lagrangians must produce at least one gluon emission if they are to give nonvanishing contributions to amplitudes. Consequently, the missing diagrams (Fig. 7) receive vanishing contributions from these Lagrangians, and these Lagrangians evade the gauge-invariance issue that we have identified in this paper. That is, the corresponding operators are truly gauge invariant.

As a further check, we have used the Lagrangians in Eqs. (33) and (35) of Ref. [8], to compute radiative jet functions in order α_s and found agreement with our results for the radiative jet functions in Sec. VII. Here, it was necessary to sum the contributions from the

order- λ operator in Eq. (33) and the \mathcal{M}_\perp order- λ^2 operator in Eq. (35) in order to obtain gauge-invariant results, in accordance with the observation in Ref. [9] that collinear gauge transformations of these Lagrangians mix operators that have different scaling in λ .

We have also used the Lagrangians in Eq. (27) of Ref. [9] to compute radiative jet functions in order α_s . Again, we have found agreement with our results for the radiative jet functions in Sec. VII. In this computation, we used the Feynman rules that are given in the erratum to Ref. [8]. In order to obtain all of the contributions to the radiative jet functions of order λ^2 , it was also necessary, in the case of these Lagrangians, to consider the order- λ correction to the gluon propagator.⁷ We derived the Feynman rule for this correction to the gluon propagator by applying the field redefinitions in Eq. (14) of Ref. [9] to the gauge-fixed gauge-field action.

IX. DISCUSSION

In this paper we have pointed out that the Lagrangians in Refs. [6, 7] (BCDF) are not gauge invariant in the hard-collinear sector. This is surprising because these Lagrangians are constructed from operators that are ostensibly gauge invariant: hard-collinear fields are accompanied by Wilson-line factors, and all derivatives are covariant derivatives. The violations of gauge invariance are somewhat subtle. They arise because hard-collinear gauge transformations multiply the quark fields by a phase that, in momentum space, can shift the quark-field momentum from the hard-collinear region to the soft region, where the hard-collinear quark field, by definition, has no support. This phenomenon is manifested in perturbation theory in the hard-collinear sector through the absence of certain diagrams that would be present in full QCD. One consequence of the absence of these diagrams is that, if one uses the BCDF Lagrangians directly to construct radiative jet functions, then the radiative jet functions are not gauge invariant by themselves.

We have demonstrated the violations of gauge invariance by examining the Ward identities for the BCDF Lagrangians and also by computing the radiative jet functions that follow directly from the BCDF Lagrangians at the leading order in g_s in the Feynman gauge and in the light-cone gauge. These analyses show that the violations of gauge invariance are, at the leading nontrivial order in g_s , proportional to inverse of the soft-quark propagator.

⁷ This contribution to the radiative jet functions corresponds to the contribution of the \mathcal{M}_\perp term in Eq. (35) of Ref. [8]. The \mathcal{M}_\perp term is absent in the Lagrangian in Eq. (27) of Ref. [9].

Motivated by the Ward-identity and radiative-jet-function analyses, we have modified the BCDF Lagrangians by adding terms that are proportional to the soft-quark equation of motion. Then, after making use of the BPS field redefinition to factor minus-polarized soft gluons from the hard-collinear subdiagram, we have arrived at gauge-invariant Lagrangians, through order λ^2 , that describe the couplings of a soft quark to a hard-collinear quark. The fact that the violations of gauge invariance can be removed through the use of a field redefinition that is proportional to the soft-quark equation of motion implies that S -matrix elements of the original BCDF Lagrangians are gauge invariant.

The modified gauge-invariant Lagrangians that we have derived are somewhat more general than the BCDF Lagrangians, in that we have considered the case of a nonzero quark mass. We have demonstrated the gauge invariance of the modified Lagrangians through examination of Ward identities in order g_s and through calculations of radiative jet functions in order α_s in the Feynman gauge and the light-cone gauge. We have also given a Ward-identity argument to show that the gauge invariance holds to all orders in g_s .

In Refs. [11, 16], the order- λ^1 Lagrangian in Eq. (13a) was used to construct a radiative jet function that involves a single-photon external state, and that radiative jet function was computed at one and two loops in perturbation theory in the light-cone gauge.⁸ As we have seen in Sec. VI, the Lagrangian in Eq. (13a) is gauge invariant to all orders in perturbation theory. Consequently, the calculations in Refs. [11, 16] are gauge invariant.

We have also examined the label-momentum formulation of SCET in the incarnations that are given in Refs. [8, 9]. The Lagrangians in these papers that describe the interactions between a soft quark and a hard-collinear quark contain commutators of covariant derivatives. Consequently, these Lagrangians must produce at least one gluon emission if they are to give nonvanishing contributions to amplitudes. It follows that the missing diagrams that correspond to these Lagrangians vanish and that the formulations of SCET in Refs. [8, 9] evade the gauge-invariance problem that we have identified in this paper.

Note added

After the present paper appeared on the arXiv, a paper [17] was submitted to the arXiv that addresses the same gauge invariance issue that we address. That paper presents the gauge-invariance issue from an alternative point of view in which the hard-collinear quark

⁸ When the transition of soft quark to a hard-collinear quark involves the emission of a single external photon, the corresponding radiative jet function of leading order in λ derives from the order- λ^1 Lagrangian in Eq. (13a). In this case, the order- λ^2 Lagrangians in Eq. (38) yield radiative jet functions that are suppressed by at least one power of λ .

fields are not constrained to carry a hard-collinear momentum.

ACKNOWLEDGMENTS

We wish to thank Martin Beneke, Philipp Böer, Hee Sok Chung, Patrick Hager, Jungil Lee, Iain Stewart, and Yunlu Wang for helpful discussions. D.K. thanks the Erwin-Schrödinger International Institute for Mathematics and Physics at the University of Vienna for partial support during the Program “Quantum Field Theory at the Frontiers of the Strong Interactions”, July 31 - September 1, 2023. X.-P. W. would like to express special thanks to the Mainz Institute for Theoretical Physics (MITP) of the Cluster of Excellence PRISMA+ (Project ID 39083149) for its hospitality and support. The work of G.T.B. is supported by the U.S. Department of Energy, Division of High Energy Physics, under Contract No. DE-AC02-06CH11357. The work of D.K. and J.-H.E. is supported by the National Key Research and Development Program of China under Contract No. 2020YFA0406301 and by the National Natural Science Foundation of China (NSFC) through Grant Nos. 12150610461, 11875112, and 12105051. The work of X.-P. W. is supported by the DFG (Deutsche Forschungsgemeinschaft, German Research Foundation) Grant No. BR 4058/2-2 and by the the DFG cluster of excellence “ORIGINS” under Germany’s Excellence Strategy - EXC-2094 - 390783311. The submitted manuscript has been created in part by UChicago Argonne, LLC, Operator of Argonne National Laboratory. Argonne, a U.S. Department of Energy Office of Science laboratory, is operated under Contract No. DE-AC02y-06CH11357. The U.S. Government retains for itself, and others acting on its behalf, a paid-up nonexclusive, irrevocable worldwide license in said article to reproduce, prepare derivative works, distribute copies to the public, and perform publicly and display publicly, by or on behalf of the Government.

All authors contributed equally to this work.

Appendix A: Derivation of the mass-dependent SCET Lagrangians

In this Appendix, we discuss the derivation of the mass-dependent Lagrangian $\mathcal{L}_{2m}^{\text{BCDF}}$ in Eq. (13). We follow the general outline of the analysis in Ref. [6], but we start with the full

QCD Lagrangian with a quark mass, namely,

$$\mathcal{L} = \bar{\psi}(i\not{D} - m)\psi. \quad (\text{A1})$$

We note that m scales as λ^2 . We decompose this Lagrangian in terms of the SCET fields, using $\psi = \xi_n + \eta_n + q_s$. Then, we use the equation of motion for the small component of the hard-collinear field η_n to eliminate η_n from the Lagrangian. This leads to the following mass-dependent Lagrangian, in addition to the terms in Eq. (34) of Ref. [6]:

$$\begin{aligned} \mathcal{L}_m = & -m\bar{q}_s q_s + m\bar{\xi}_n \frac{1}{i\bar{n} \cdot D} \frac{\not{n}}{2} i\not{D}_\perp \xi_n + m\bar{\xi}_n i\not{D}_\perp \frac{1}{i\bar{n} \cdot D} \frac{\not{n}}{2} \xi_n \\ & -m^2 \bar{\xi}_n \frac{1}{i\bar{n} \cdot D} \frac{\not{n}}{2} \xi_n + m\bar{\xi}_n \frac{1}{i\bar{n} \cdot D} g_s \bar{n} \cdot G_n q_s + m\bar{q}_s g_s \bar{n} \cdot G_n \frac{1}{i\bar{n} \cdot D} \xi_n \\ & + m\bar{\xi}_n \frac{1}{i\bar{n} \cdot D} \frac{\not{n}}{2} g_s \not{G}_{n\perp} q_s + m\bar{q}_s g_s \not{G}_{n\perp} \frac{1}{i\bar{n} \cdot D} \frac{\not{n}}{2} \xi, \end{aligned} \quad (\text{A2})$$

where

$$\begin{aligned} i\bar{n} \cdot D &= i\bar{n} \cdot \partial + g_s \bar{n} \cdot G_n + g_s \bar{n} \cdot G_s, \\ iD_\perp^\mu &= iD_{n\perp}^\mu + g_s G_{s\perp}^\mu. \end{aligned} \quad (\text{A3})$$

The first term of Eq. (A2) gives the order- λ^0 contribution to the action, and it yields the mass term of the leading-power soft-quark Lagrangian

$$\mathcal{L}_s^{(0)} = \bar{q}_s (i\not{D}_s - m) q_s. \quad (\text{A4})$$

Note that the second and third terms on the right side of Eq. (A2) are of order λ or smaller, while the fourth through sixth terms are of order λ^2 , and the seventh and eighth terms are of order λ^3 .

Next, let us perform the expansions in powers of λ that are required for homogeneous scaling for each term of the Lagrangian. We can accomplish this by making use of the identity in Eq. (36) of Ref. [6],

$$\frac{1}{i\bar{n} \cdot D} g_s \bar{n} \cdot G_n q_s = (1 - WZ^\dagger) q_s - \frac{1}{i\bar{n} \cdot D} (1 - WZ^\dagger) i\bar{n} \cdot D_s q_s, \quad (\text{A5})$$

and the power expansions of the Wilson lines and the covariant derivatives,

$$\begin{aligned}
WZ^\dagger &= W_n [1 + O(\lambda^2)], \\
\frac{1}{i\bar{n} \cdot D} &= \frac{1}{i\bar{n} \cdot D_n} [1 + O(\lambda^2)], \\
iD_\perp^\mu &= iD_{n\perp}^\mu [1 + O(\lambda)],
\end{aligned} \tag{A6}$$

where we have given the relative orders in λ of the corrections. Then, through order λ^2 , we obtain the following mass-dependent Lagrangians:

$$\begin{aligned}
\mathcal{L}_m^{(0)} &= -m\bar{q}_s q_s, \\
\mathcal{L}_m^{(1)} &= m\bar{\xi}_n \frac{1}{i\bar{n} \cdot D_n} \frac{\not{n}}{2} i\not{D}_{n\perp} \xi_n + m\bar{\xi}_n i\not{D}_{n\perp} \frac{1}{i\bar{n} \cdot D_n} \frac{\not{n}}{2} \xi_n, \\
\mathcal{L}_m^{(2)} &= -m^2 \bar{\xi}_n \frac{1}{i\bar{n} \cdot D_n} \frac{\not{n}}{2} \xi_n - m\bar{q}_s W_n^\dagger \xi_n - m\bar{\xi}_n W_n q_s.
\end{aligned} \tag{A7}$$

Here, in order to ensure homogeneous scaling in λ , one should multipole expand the position arguments of q_s and \bar{q}_s in $\mathcal{L}_m^{(2)}$ as follows:

$$q_s(x) = q_s(x^+) + [(x_\perp \cdot \partial_\perp) q_s](x^+) + O(\lambda^2 q_s). \tag{A8}$$

Note that the mass terms in $\mathcal{L}_m^{(1)}$ and the first term of $\mathcal{L}_m^{(2)}$ would have given the mass term of the leading-power SCET Lagrangian if we had used the power counting $m \sim \lambda$, rather than $m \sim \lambda^2$, as would be appropriate for collinear modes, rather than hard-collinear modes. This would have led to the following leading-power Lagrangian:

$$\mathcal{L}_n^{(0)}|_{m \sim O(\lambda)} = \bar{\xi}_n \left[i\bar{n} \cdot D_n + (i\not{D}_{n\perp} - m) \frac{1}{i\bar{n} \cdot D_n} (i\not{D}_{n\perp} + m) \right] \frac{\not{n}}{2} \xi_n. \tag{A9}$$

Appendix B: Power suppressed diagrams of $A(\ell^-)$ in Feynman gauge

In this Appendix, we show that the diagrams of Figs. 5(a) and (d) lead to power-suppressed contributions in the Feynman gauge.

The diagram of Fig. 5(a) gives

$$\begin{aligned}
& A_{(a),\text{Feynman}}(\ell^-) \\
&= (T^e)^{bc}(T^e)^{da} \left\{ \left(-n \cdot p \frac{\not{n}}{2} \right) P_n \Pi_{3S_1^{[1]}}^{cd}(ig_s \gamma_\mu) \frac{i}{2\not{p} - \not{\ell} - m + i\varepsilon} P_{\bar{n}} \right\}^{\beta\alpha} \frac{i(-ig_s \bar{n}^\mu)}{\bar{n} \cdot (p - \ell) + i\varepsilon} \frac{-i}{(p - \ell)^2 + i\varepsilon} \\
&= -\frac{ig_s^2 C_F \delta^{ba}}{\sqrt{2N_c} mp^+} \frac{1}{(-\ell^- + i\varepsilon)} \left(\frac{\not{n} \not{\ell} \not{\ell}^*}{4} \right)^{\beta\alpha} \frac{p^-}{(-\ell^- + i\varepsilon)}, \tag{B1}
\end{aligned}$$

where we have kept only the leading nonzero power in λ in the last line, which, in effect, enforces the multipole expansion. Here, we are using the scalings with λ of ℓ and p that are given in Eqs. (5) and (25), respectively. We see that the expression in Eq. (B1) has an additional power λ^2 relative to the contribution in Eq. (27). That is, it is power suppressed.

The diagram of Fig. 5(d) gives

$$\begin{aligned}
& A_{(d),\text{Feynman}}(\ell^-) \\
&= (T^e)^{bc}(T^e)^{da} \left\{ g_s \left(n_\mu + \gamma_{\perp\mu} \frac{\not{p}_\perp}{\bar{n} \cdot p} \right) P_n \Pi_{3S_1^{[1]}}^{cd}(ig_s \gamma^\mu) \frac{i}{2\not{p} - \not{\ell} - m + i\varepsilon} P_{\bar{n}} \right\}^{\beta\alpha} \frac{-i}{(p - \ell)^2 + i\varepsilon} \\
&= -\frac{ig_s^2 C_F \delta^{ba}}{\sqrt{2N_c} mp^+} \frac{1}{(-\ell^- + i\varepsilon)} \frac{-m^2 \left(\frac{\not{n} \not{\ell} \not{\ell}^*}{4} \right)^{\beta\alpha} + m \left(\frac{\not{n} \not{\ell} \not{\ell}^* \not{\ell}_\perp}{4} \right)^{\beta\alpha}}{2p^+(-\ell^- + i\varepsilon)}, \tag{B2}
\end{aligned}$$

where we have kept only the leading nonzero power in λ in the last line. Again, we are using the scalings with λ of ℓ and p that are given in Eqs. (5) and (25), respectively. The expression in Eq. (B2) has an additional power λ^2 relative to the contribution in Eq. (27). That is, it is power suppressed.

-
- [1] C. W. Bauer, S. Fleming and M. E. Luke, Summing Sudakov logarithms in $B \rightarrow X_s \gamma$ in effective field theory, Phys. Rev. D **63**, 014006 (2000) [arXiv:hep-ph/0005275 [hep-ph]].
- [2] C. W. Bauer, S. Fleming, D. Pirjol and I. W. Stewart, An Effective field theory for collinear and soft gluons: Heavy to light decays, Phys. Rev. D **63**, 114020 (2001) [arXiv:hep-ph/0011336 [hep-ph]].
- [3] C. W. Bauer and I. W. Stewart, Invariant operators in collinear effective theory, Phys. Lett. B **516**, 134-142 (2001) [arXiv:hep-ph/0107001 [hep-ph]].

- [4] C. W. Bauer, D. Pirjol and I. W. Stewart, Soft collinear factorization in effective field theory, *Phys. Rev. D* **65**, 054022 (2002) [arXiv:hep-ph/0109045 [hep-ph]].
- [5] C. W. Bauer, S. Fleming, D. Pirjol, I. Z. Rothstein and I. W. Stewart, Hard scattering factorization from effective field theory, *Phys. Rev. D* **66**, 014017 (2002) [arXiv:hep-ph/0202088 [hep-ph]].
- [6] M. Beneke, A. P. Chapovsky, M. Diehl and T. Feldmann, Soft collinear effective theory and heavy to light currents beyond leading power, *Nucl. Phys. B* **643**, 431-476 (2002) [arXiv:hep-ph/0206152 [hep-ph]].
- [7] M. Beneke and T. Feldmann, Multipole expanded soft collinear effective theory with non-Abelian gauge symmetry, *Phys. Lett. B* **553**, 267-276 (2003) [arXiv:hep-ph/0211358 [hep-ph]].
- [8] D. Pirjol and I. W. Stewart, A Complete basis for power suppressed collinear ultrasoft operators, *Phys. Rev. D* **67**, 094005 (2003) [erratum: *Phys. Rev. D* **69**, 019903 (2004)] [arXiv:hep-ph/0211251 [hep-ph]].
- [9] C. W. Bauer, D. Pirjol and I. W. Stewart, On Power suppressed operators and gauge invariance in SCET, *Phys. Rev. D* **68**, 034021 (2003) [arXiv:hep-ph/0303156 [hep-ph]].
- [10] I. Moutl, I. W. Stewart and G. Vita, Subleading Power Factorization with Radiative Functions, *JHEP* **11**, 153 (2019) [arXiv:1905.07411 [hep-ph]].
- [11] Z. L. Liu and M. Neubert, Factorization at subleading power and endpoint-divergent convolutions in $h \rightarrow \gamma\gamma$ decay, *JHEP* **04**, 033 (2020) [arXiv:1912.08818 [hep-ph]].
- [12] M. Beneke, A. Broggio, S. Jaskiewicz and L. Vernazza, Threshold factorization of the Drell-Yan process at next-to-leading power, *JHEP* **07**, 078 (2020) [arXiv:1912.01585 [hep-ph]].
- [13] See, for example, C. Arzt, Reduced effective Lagrangians, *Phys. Lett. B* **342**, 189-195 (1995) [arXiv:hep-ph/9304230 [hep-ph]], and references therein.
- [14] G. Grammer, Jr. and D. R. Yennie, Improved treatment for the infrared divergence problem in quantum electrodynamics, *Phys. Rev. D* **8**, 4332 (1973).
- [15] J. C. Collins, D. E. Soper, and G. F. Sterman, Soft gluons and factorization, *Nucl. Phys. B* **308**, 833 (1988).
- [16] Z. L. Liu and M. Neubert, Two-Loop Radiative Jet Function for Exclusive B -Meson and Higgs Decays, *JHEP* **06**, 060 (2020) [arXiv:2003.03393 [hep-ph]].
- [17] P. Böer and P. Hager, On the gauge-invariance of SCET beyond leading power, *JHEP* **08**, 197 (2023) [arXiv:2306.12412 [hep-ph]].